http://dx.doi.org/10.5935/0103-5053.20130043
J. Braz. Chem. Soc., Vol. 24, No. 2, 336-343, 2013.
Printed in Brazil - ©2013 Sociedade Brasileira de Química
0103 - 5053 $6.00+0.00

Article

Hosted Formation of PbS Crystals on Polyethylene Modified Surface

*Vanessa H. Fragal,[a] Rafael Silva,[b] Thelma P. Cellet,[a] Guilherme M. Pereira,[a]
Marcos H. Kunita,[a] Edvani C. Muniz[a] and Adley F. Rubira*,[a]*

*[a]Departamento de Química, Universidade Estadual de Maringá,
Av. Colombo, 5790, 87020-900 Maringá-PR, Brazil*

*[b]Department of Chemistry and Chemical Biology, Rutgers, The State University of New Jersey,
610 Taylor Road, Piscataway, NJ 08854, USA*

Nanocristais inorgânicos estáveis e suportados, como PbS ou outros *quantum dots*, são materiais extremamente importantes quando obtidos na forma de filmes finos para a aplicação em áreas tecnológicas. Neste trabalho, um método para o crescimento de cristais de PbS sobre filme ultrafino de poli(ácido acrílico) (PAA) covalentemente imobilizado na superfície de polietileno (PE) é descrito. O método utilizado permite a obtenção de materiais com diferentes formas e tamanhos pelo ajuste de variáveis experimentais. Os compostos mais homogêneos e com as menores partículas foram obtidos em pH 6 devido a remoção mais lenta de íons Pb^{2+} adsorvidos no filme ultrafino de PAA. Dessa forma, o PbS é formado *in situ* no interior do PAA. A análise da morfologia dos compósitos mostrou uma relação direta entre a concentração de Pb^{2+} e a concentração de tioacetamida (TAA). Compósitos mais homogêneos com as partículas menores foram obtidos na condição de menor concentração de Pb^{2+} e maior concentração de TAA ou na condição intermediária de Pb^{2+} e menor concentração de TAA.

Supported and stable inorganic crystals in nanometric size, such as PbS or other quantum dots, are very desired materials in the form of thin films for the application in technological areas. Herein, an approach to the growth of PbS crystals in poly(acrylic acid) (PAA) ultrathin film covalently immobilized in the polyethylene (PE) surface is described. The method used allows the obtaining of materials with different shapes and sizes by the adjustment of experimental variables. The more homogenous composites with the smallest particles were obtained at pH 6 due to the slower removal of Pb^{2+} ions from PAA ultrathin film. Hence, the PbS is formed *in situ* inside of PAA. A direct relationship between Pb^{2+} and thioacetamide (TAA) concentrations was observed by the analysis of the composite morphologies. More homogenous composites with the smallest particles were obtained in the lowest Pb^{2+} condition and the highest TAA concentration condition or in the intermediate Pb^{2+} condition and the lowest TAA concentration condition.

Keywords: polyethylene ultrathin polymer layers, PbS quantum dots, PbS nanoparticles

Introduction

The development of technical applications exploring semiconductor nanocrystal (quantum dots, QDs) properties is one of the most debated subjects on nanotechnology in the last years.[1-3] QDs are attractive materials mainly as a function of their optical properties, which can be adjusted as function of composition, size, shape and surface characteristics of QDs.[4] QDs have great potential in light emission diodes, biologic labeling, sensors, solar cells and medical imaging. Since QDs have high superficial areas, superficial defects are relevant toward energetic states, affecting their chemical and physical properties.[5] Therefore, the utilization of host material in the synthesis of QDs has a double rule. The host material acts as a capping agent, preventing the aggregation of the crystals, and the host materials can also interact with the surface of QDs altering their general properties.[6,7] Ligand of QDs changes their band-edge and quantum yield in different solvents, altering the behavior of QDs in different medium, which are correlated with the characteristic of the materials used in the surface modification of QDs.[8,9] Thus, surface ligands passivate the QD surface states and provide colloidal stability (solubility) in nonpolar organic solvents.[10,11]

---

*e-mail: afrubira@uem.br

Stabilization and formation of films with QDs are important challenges in the nanotechnology development. The reproduction of the properties exhibited by QDs colloidal system in solid system is a significant task in the utilization of QDs such as those used in the fields of solar cells, infrared imaging and so on.[12,13] In this way, the incorporation of nanoparticles in solid hosts is a good approach.[14,15]

Several techniques were reported exemplifying the formation or immobilization of nanoparticle in solid materials, mainly polymeric host, which provides homogenous composites avoiding the aggregation of the particles.[16] While the immobilization of QDs in solid host can prevent the aggregation, the exploration of the optical properties of QDs turns out to be more problematic in function of the host light absorption. One alternative that is proposed in the present work is the immobilization of QDs into ultrathin polymeric layer, which can be created on the surface of common solid substrates.

The formation of ultrathin polymeric layer supported on solid substrate by suitable methods promises the modification and improvement of the surface characteristics of the substrate without alteration of the bulk characteristic.[17] Methods exploring common polymer substrates, as for example polyethylene (PE), are used in the development of ultrathin layer of polyfunctional polymers.[18-20]

PE substrate was chosen in this study because it is an attractive material for the preparation of composites due to interesting bulk properties such as malleability. In addition, the easy processing of PE allows low cost fabrication of devices with controlled dimensions and shape. Thus, composite materials with suitable optical properties have been obtained by using low cost raw materials and polyethylene substrate with chemically modified surfaces.

Ultrathin layer can be used as a special chemical ambient for the synthesis of nanoparticles. Silva *et al.*[21] demonstrated the preparation of calcium carbonate in ultrathin layers deposited on polyethylene films in order to prepare biocompatible surface. The authors claimed the chemical ambient in the solid layers has influences on the characteristic of the crystals formed acting in the stabilization of more energetic phases.

Among the most studied QDs, PbS has a special features; a large exciton Bohr radius of 18 nm and hence shows strong quantum size effects for relatively large sizes as compared to other semiconductors, such as CdS, CdSe and ZnS.[22,23] PbS quantum dots exhibit about 300% quantum efficiency due to multiple exciton generation.[24] PbS exhibits near-infrared photoluminescence (PL) emission, which makes PbS a potential material for application in telecommunication and in biotechnology.[25] Further nanocomposites of PbS have exceptional third order nonlinear properties.[26,27]

During the past few years, many efforts have been devoted to synthesize microcrystal or nanocrystal of PbS. Many works deposited on the glass films of PbS using the successive ionic layer adsorption and reaction method or deposition bath.[28-30] However, they do not employ strategically modified substrates with thin polymer layers to complex the ions Pb^{+2} enabling a control arrangement and morphology of the nano or microcrystal during the synthesis process.

In the present work, the formation of PbS particles on the surface of PE modified with a poly(acrylic acid) (PAA) ultrathin layer is discussed. Scheme 1 illustrates the general principle of this process. PAA, a polyfunctional polymer, was chosen on the basis of its capacity for retaining lead ions, as a polycarboxylate, and strong coordination ability to the PbS QD surfaces as a multidentate ligand. PbS was formed *in situ* using thioacetamide (TAA) as precursor of the sulfide.

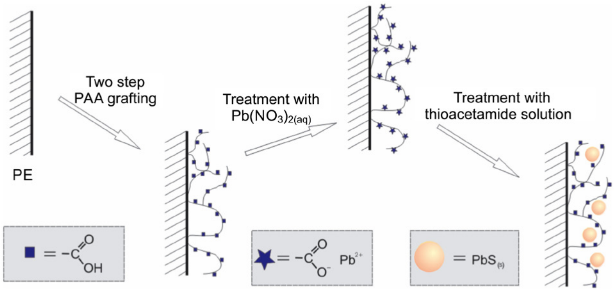

Scheme 1. Schematic representation of the formation of the ultrathin layer of PAA on the PE surface and the use of PAA to produce PbS in the ultrathin layer.

Experimental

PE substrate

The substrate was prepared according to a procedure previously presented.[16] Briefly, PE films were prepared using low density polyethylene (LDPE) pellets (Aldrich). PE pellets were converted into 3.0 × 4.0 cm films with mean width of 0.380 mm. PE films were cleaned in Soxhlet using acetone.

PAA ultrathin layer

PE films were oxidized in 1.5 mol L^{-1} chromic acid solution for 5 min under controlled temperature at 70 ºC. Oxidized films were used to anchor a poly(vinyl alcohol) (PVA) layer by thermal esterification. Oxidized films were placed in Petri dishes and recovered by a 5% (m/v) aqueous

PVA solution (PVA, 88% hydrolyzed and Mw ranging from 13000 to 23000). The Petri dishes were kept in an oven for 24 h at 70 ºC and 1 h at 140 ºC. After the thermal treatment, the samples were submitted to extraction in Soxhlet for 12 h using distilled water in order to extract the PVA not bound to the substrate surface. After the immobilization of PVA, PAA was immobilized in the film previously modified with PVA. The procedure for the PAA immobilization is very similar to the PVA process. Films modified with PVA were placed in Petri dishes and recovered with a 5% (m/v) aqueous PAA solution (Mw 15200 g mol^{-1}). Petri dishes, containing the films immersed in the solutions, were heated in an oven at 70 ºC for 24 h and after 140 ºC for 1 h. The removal of PAA not bound to the films was carried out in a Soxhlet using water for 24 h.

Pb(II) ion chelating

Films containing PAA ultrathin layer immobilized on the PE films were immersed in $Pb(NO_3)_2$ solutions for 24 h at 60 °C. In order to analyze the influence of the solution concentration, different solutions were used with different concentrations. After the treatment in the $Pb(NO_3)_2$ solutions, films were washed in distilled water and dried in vacuum atmosphere.

In situ PbS formation

Formation of PbS from the Pb(II) ions chelated in PAA was carried out using thioacetamide (TAA) solutions. Films modified with PAA were immersed in TAA solution for 4 h at 60 °C. TAA concentration and pH values were controlled and the influence of these factors was studied in the present work. Hydrochloric acid (HCl) was added in order to adjust the pH of the solution.

Characterizations

The formation of the ultrathin layer containing lead ions and the formation of PbS were characterized by attenuated total reflection in Fourier transform infrared spectroscopy (ATR-FTIR) using Bomem model MB-100 equipped with a Pike MIRacle ATR accessory at an incident angle of 45° and a ZnSe crystal under nitrogen stream. UV-Vis spectroscopy was obtained by UV-Vis spectrophotometer (Shimadzu, UV mini 1240). X-ray diffractograms (XRD) were obtained in D-6000 Shimadzu using a Cu line $K_\alpha = 1.5406$ Å. The diffractograms were obtained in the following conditions: 2θ range of 25-60°, 35 kV, 18 mA, counting time of 1 s, 0.5° min^{-1}, and slit width of 0.05 mm. Morphological characterization was performed in a scanning electron microscope (Shimadzu, model SS 550 Superscan). SEM images were made applying an accelerating voltage of 10 kV and a current intensity of 30 μA.

Results and Discussion

The substrate used in the PbS synthesis has a high density of carboxylic groups on its surface as evidenced by the band at 1720 cm^{-1} in the ATR-FTIR spectrum (Figure 1). This band is attributed to the carbonyls of PAA and the carbonyls of the ester groups of the cross-linkage between PAA and PVA, as well as to the ester groups formed by the linkage between PVA and the functional groups on the surface of PE.

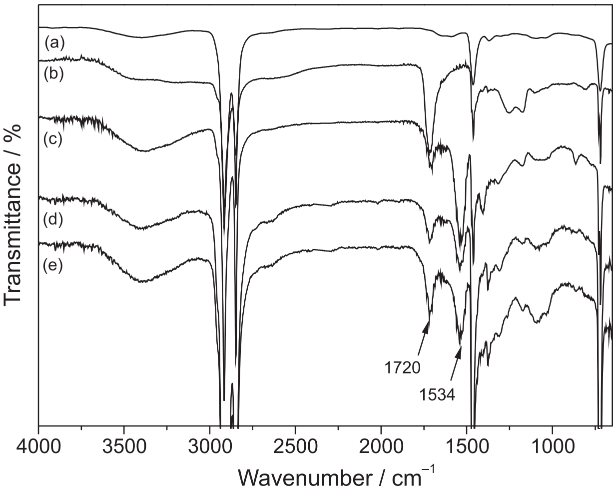

Figure 1. ATR-FTIR spectra of (a) pristine PE, (b) PE after the imobilization of PVA and PAA (PE/PAA), PE/PAA treated with (c) 0.15, (d) 0.75 and (e) 1.50 mol L^{-1} $Pb(NO_3)_2$.

PE films with PAA immobilized on the surface were immersed in Pb^{2+} solutions. In these solutions, the retention of the Pb^{2+} ions by the film occurs due to the partial neutralization of the carboxylic acid groups from PAA on the substrate surface. This statement can be confirmed by the appearance of a band at 1534 cm^{-1} in the FTIR spectra of the films treated with lead solution in different concentrations, Figure 1 (curves c, d and e). The band at 1534 cm^{-1} is attributed to the carbonyl band in carboxylate groups formed by the neutralization of the carboxylic acid groups by the lead solution.

The films were immersed in TAA solutions after the deposition of lead ions on the film surfaces. During this period, the TAA thermal decomposition occurs, generating hydrogen sulfide and consequently, as function of the dissociation equilibrium, sulfide ions are generated in the solution. Two different processes occur in the film surface; the acid media provoke the protonation of the carboxylate group and sulfide ions cause the precipitation of the lead as PbS.

The characteristics of the particles formed on the surface depend on the relation between these two processes. In Figures 2 and 3, it can be verified the FTIR spectra of the films after the treatment with TAA at pH 2 and 6, respectively. In both cases, it is observed that the band attributed to the carboxylate ion (in 1534 cm^{-1}) disappeared, indicating the conversion of the carboxylate to carboxylic acid group.

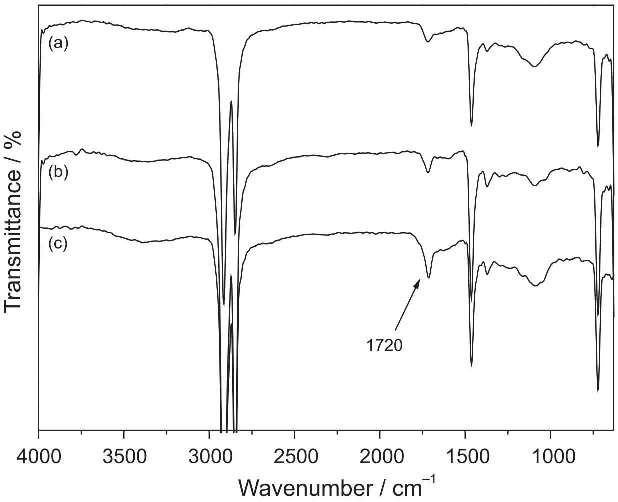

Figure 2. ATR-FTIR spectra of samples after the TAA treatment using pH 2 and 0.5 mol L^{-1} TAA from samples obtained in different Pb(NO$_3$)$_2$ concentrations: (a) 0.15, (b) 0.75 and (c) 1.50 mol L^{-1}.

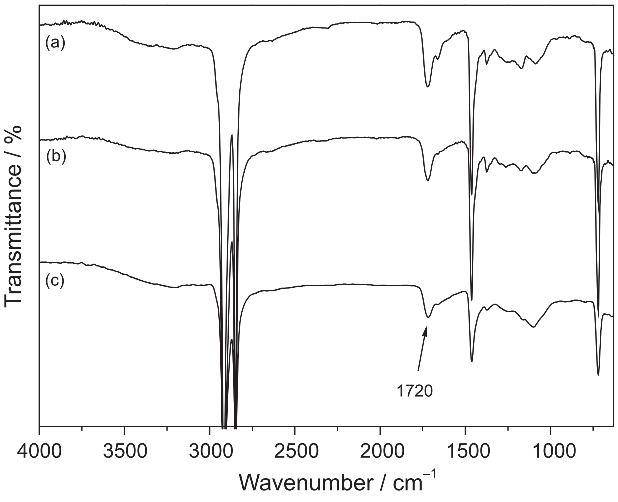

Figure 3. ATR-FTIR spectra of samples after the TAA treatment using pH 6 and 0.5 mol L^{-1} TAA from samples obtained in different Pb(NO$_3$)$_2$ concentrations: (a) 0.15, (b) 0.75 and (c) 1.50 mol L^{-1}.

The variation of the surface morphology of the substrate can be analyzed in all steps of the process using the SEM micrographs. In Figure 4a, it can be seen the micrograph of the substrate containing the PAA layer immobilized. The PE/PAA film has very homogeneous surface. The immersion of the PE/PAA film in the lead solution causes the modification of its morphology. In the SEM micrographs presented in Figures 4b, 4c and 4d, it is verified that the surfaces of the films are more rough and heterogeneous. It is consequence of the modification of the carboxylic acid groups to carboxylate groups as verified by FTIR analysis.

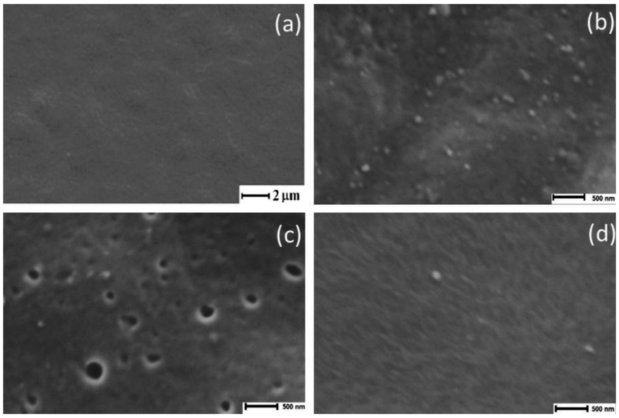

Figure 4. SEM micrographs of (a) PE after the imobilization of PVA and PAA (PE/PAA) and PE/PAA treated with (b) 0.15, (c) 0.75 and (d) 1.50 mol L^{-1} Pb(NO$_3$)$_2$.

The formation of the PbS particles on the surface of the substrate is easily verified in the micrographs of the films after treatment with TAA, SEM micrographs are presented in Figures 5, 6 and 7. Observing Figures 5, 6 and 7, it is verified the formation of particles and clusters uniformly spread over the surfaces of the films. The surface morphologies of the composites are very diverse, indicating that the synthesis variables are important in the final configuration of the composite, mainly in the recovery degree and in the size of the PbS particles. The variables analyzed are lead ion concentration, TAA concentration and pH value of the TAA solution.

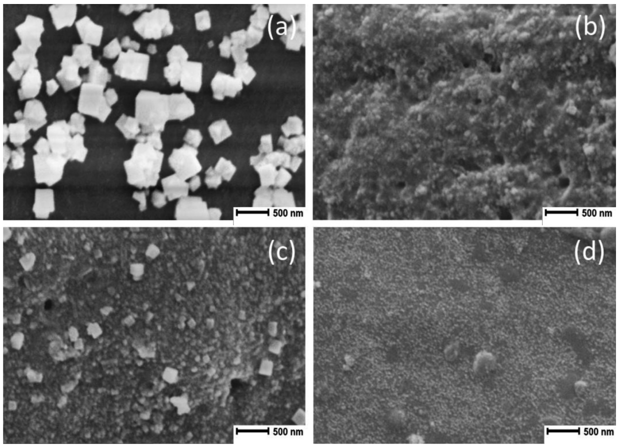

Figure 5. SEM micrographs of PE/PbS films obtained using the PE/PAA film treated with Pb(NO$_3$)$_2$ 0.15 mol L^{-1}. TAA treatment condition: (a) TAA 0.005 mol L^{-1} and pH 2; (b) TAA 0.005 mol L^{-1} and pH 6; (c) TAA 0.5 mol L^{-1} and pH 2; and (d) TAA 0.5 mol L^{-1} and pH 6.

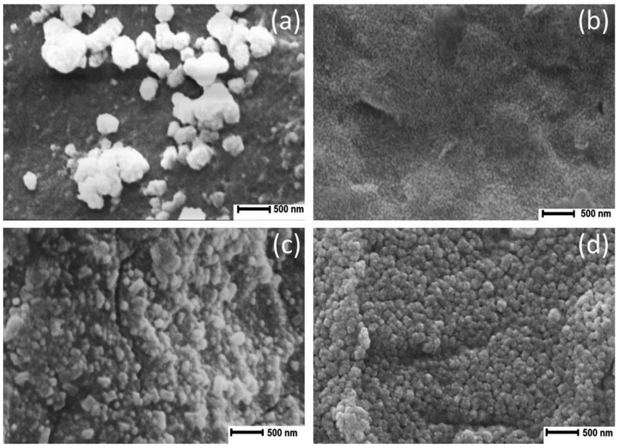

Figure 6. SEM micrographs of PE/PbS films obtained using the PE/PAA film treated with $Pb(NO_3)_2$ 0.75 mol L^{-1}. TAA treatment condition: (a) TAA 0.005 mol L^{-1} and pH 2; (b) TAA 0.005 mol L^{-1} and pH 6; (c) TAA 0.5 mol L^{-1} and pH 2; and (d) TAA 0.5 mol L^{-1} and pH 6.

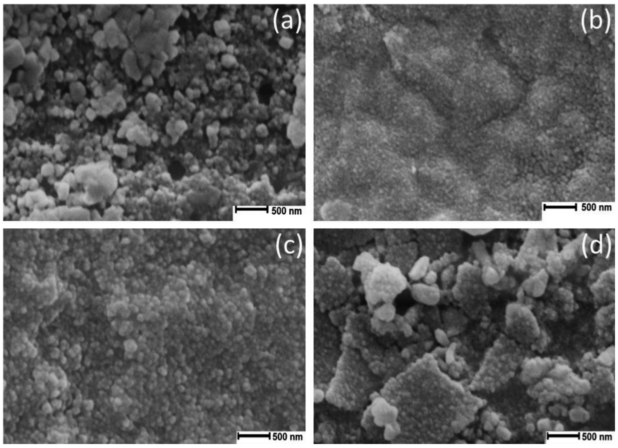

Figure 7. SEM micrographs of PE/PbS films obtained using the PE/PAA film treated with $Pb(NO_3)_2$ 1.5 mol L^{-1}. TAA treatment condition: (a) TAA 0.005 mol L^{-1} and pH 2; (b) TAA 0.005 mol L^{-1} and pH 6; (c) TAA 0.5 mol L^{-1} and pH 2; and (d) TAA 0.5 mol L^{-1} and pH 6.

The amount of material formed on the surface of the substrate can be adjusted by the concentration of Pb^{2+} in the solution. Three different solutions were used with the following Pb^{2+} concentration: 0.15, 0.75 and 1.5 mol L^{-1}. Comparing the groups of samples in Figure 5 with the group of samples in Figure 6, it can be affirmed that the increase of the solution concentration from 0.15 to 0.75 mol L^{-1} caused the increase in the density of particles in the surface of the film. It is more clearly verified comparing the SEM micrographs in Figures 5d and 6d. Besides the increase in the density of particles in the surface (Figures 5d to 6d), it is also verified the increase of the size of particles.

The samples with SEM micrographs presented in Figures 5a and 6a were prepared under the same TAA treatment condition, but from different concentration of Pb^{2+}. In the sample from the more diluted Pb^{2+} solution (Figure 5a), it is observed that PbS are more uniform with shape resembling cubic crystals. However, PbS crystals prepared from 0.75 mol L^{-1} Pb^{2+} have an irregular shape and size as a result of the agglomeration of the crystal during the growth. This tendency is strongly observed in the SEM micrographs of the composites prepared from the more concentrated solution (Figure 7), in which all the surface of the films are recovered with PbS crystals agglomerated.

Variables in the TAA treatment (TAA concentration and pH value) cause severe alteration in the PbS crystal formed. Two different pH were used, 2 and 6. The influence of the pH can be noted comparing Figure 5a with Figure 5b or Figure 5c with Figure 5d. In the more acid condition, the particles are bigger and more uncovered. The acid concentration participates increasing the speed of sulfide ion formation and also in the protonation of the carboxylate ions and removal of the Pb^{2+} ions from the PAA layer. In this manner, the formation of PbS occurs more in the solution when Pb^{2+} is released, causing the PbS precipitation over the film. At pH 6, the protonation of the carboxylic acid is a process that occurs during the formation of the hydrogen sulfide. Thus, the formation of PbS occurs mainly inside of the PAA layer. Consequently, PAA acts as a capping agent controlling the PbS growth. Therefore, in Figures 6 and 7, it can be verified that the samples prepared at pH 6 (curves b and d) have been more uniformly coated in comparison with the samples prepared at pH 2.

The variation of TAA concentration promoted changes in the concentration of the sulfide ion in solution. The composites were prepared using two different conditions (0.005 and 0.5 mol L^{-1}). The increase of TAA concentration increases the nucleation rate, resulting in the decrease of the particle mean size for the films with the lowest Pb^{2+} concentration. This statement is visibly verified comparing the Figure 5a with Figure 5c or Figure 5b with Figure 5d. However, it is also observed that the increase in the TAA concentration, for the condition of high Pb^{2+} concentration, increases the amount of PbS in the surface of the films, favoring the aggregation of the PbS particles (Figures 6 and 7).

Comparing the SEM micrographs in Figures 5, 6 and 7, it is affirmed that there is a direct relationship between Pb^{2+} concentration and TAA concentration because the more homogenous composites with the smallest particles were obtained in the lowest Pb^{2+} concentration condition and the higher TAA concentration condition or in the intermediate Pb^{2+} condition and the lowest TAA concentration condition.

The presence of the PbS phase on the surface of substrate after the immersion of the films in the TAA solution was confirmed by X-ray diffraction analysis, as shown in Figure 8. The diffractogram observed in Figure 8 shows the simple superposition of the signals from PbS and polyethylene. The highlighted signals in the diffractogram are characteristic signals of the PbS crystalline phase (JCPDS card 01-0880) and all other signals are attributed to PE (JCPDS card 11-0834). The X-ray diffraction patterns indicate the samples are well crystallized.

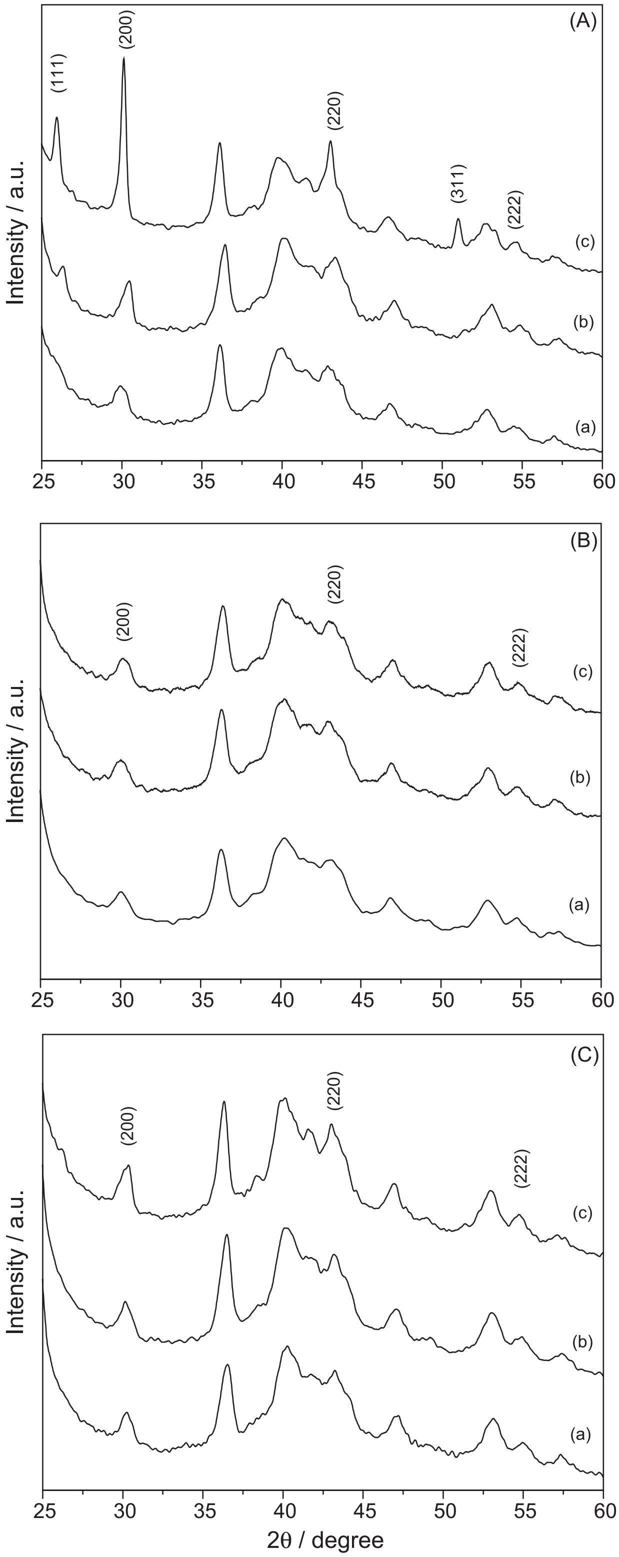

Figure 8. XRD diffractograms of the PbS immobilized in the surface of polyethylene film. Samples prepared by the following conditions (a) 0.15, (b) 0.75 and (c) 1.5 mol L^{-1} Pb(NO$_3$)$_2$; (A): TAA 0.5 mol L^{-1} and pH 2; (B) TAA 0.5 mol L^{-1}and pH 6; and (C) TAA 0.005 mol L^{-1} and pH 2.

Figure 8A shows that the increase of the concentration of Pb^{+2} directly influences on the quantity and clarity of the signals in diffractograms. The highest concentration of Pb^{+2} generated more crystalline PbS, forming narrower peaks. By the comparison of Figures 8A and 8B, it is observed the PbS peaks (pH 6) are less intense and narrow, demonstrating that the best crystal was formed at pH 2. In such a condition, the crystal formation can be slower because the bigger particles are formed and the surface of the film is more uncovered than that at pH 6. The decrease in concentration of TAA (Figure 8C) does not generate crystals highly structured, comparatively to higher concentrations of TAA (Figure 8A). This fact can also be verified by SEM micrographs (Figure 5). Thus, the increase of the nucleation rate decreases both the mean size of the particles and the crystallinity of PbS.

The film composites obtained from the lowest Pb^{2+} and the biggest Pb^{2+} concentrations were analyzed by UV-Vis spectroscopy. The spectra can be visualized in Figure 9. In the spectra of the composites, it is verified that the composite films present an additional broad and intense bands at 250 and 280 nm, compared to the precursor film doped with Pb^{2+}. These bands are attributed to the absorption of the transitions 1p$_e$-1p$_h$ of PbS crystal in the surface of the films.

The more homogeneous samples with intermediate sizes (Figures 5 and 7, curves d) show a main absorption at 280 nm (Figures 9A and 9B, curves e). The samples with smaller particle sizes have absorbance at about 250 nm. In the spectra in Figures 9A and 9B, curves d, it is observed the appearance of bands at 250 and 290 nm. From both the spectrum of Figure 9B, curve d, and the SEM micrograph in Figure 7c, it could be said that there are two populations of particles: a minor population with smaller sizes and a larger population with larger size. Conversely, in Figure 9A, curve d, there are a larger population with smaller sizes and a minor population with larger sizes (Figure 5c). In Figure 9A, curve c, there is a wide distribution of particle size which results in a broad band that absorbs at the spectral region of 250 to 290 nm (Figure 5b). The particles with larger sizes (Figure 7a and 7b) hardly absorbed at the scanned wavelength, shown in Figure 9B, curves b and c.

One important fact is the absence of this band only in the film obtained with the more acid pH, 2, and the lowest TAA concentration, 0.005 mol L^{-1}. However, when this result is related with the morphology of the composites in Figure 5, it can be realized that this particular sample presents the PbS particles with a very different morphology, cubic, and

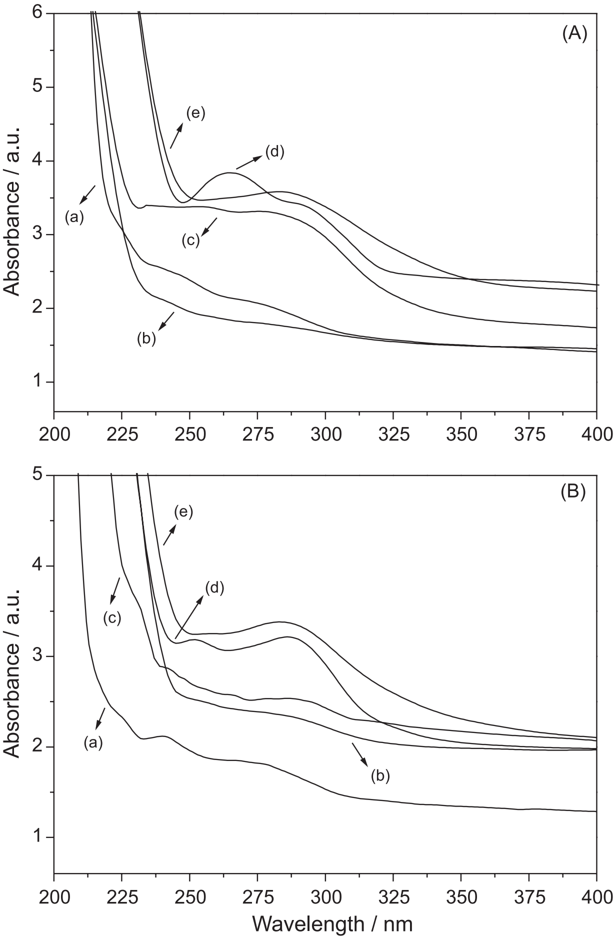

Figure 9. UV-Vis spectroscopy of PE/PAA treated with (A) 0.15 and (B) 1.5 mol L^{-1} Pb(NO$_3$)$_2$; (a) precursor film; (b) 0.005 mol L^{-1} TAA and pH 2; (c) 0.005 mol L^{-1} TAA and pH 6; (d) 0.5 mol L^{-1} TAA and pH 2; (e) and 0.5 mol L^{-1} TAA and pH 6.

the particles are bigger than particles observed in the other composites, indicating that the absorption band is not only related to the presence of PbS, but also to the characteristic size and shape of the crystal.

The appearance of all PE films is similar each to other and may prove the synthesis of PbS on PE (Figure 10) because the films closely resemble the galena (PbS), which also presents a silver color.

Figure 10. Photo of PE film immobilized with PbS with 0.75 mol L^{-1} Pb(NO$_3$)$_2$, TAA 0.005 mol L^{-1} and pH 6.

Conclusion

PbS crystals can be prepared *in situ* on the surface of a polymeric substrate using the methodology of immobilization of an ultrathin PAA layer. The morphology of the composite formed in relation to the amount of PbS particles as well as the size and the shape of the PbS particles can be adjusted by controlling the variables of the system.

The Pb^{2+} concentration, TAA concentration and pH variables of the TAA solution have a high influence in the growth of the PbS crystal, which can be synthetized the according to the possible application. The selection of the variables by the method presented here can tune the size of the nanoparticles from nano to micrometric.

The more homogenous composites with the smallest particles were obtained in higher pH condition due to the slower removal of Pb^{2+} ions from PAA ultrathin film and hence PbS is formed inside of PAA. In addition, analyzing the composites morphology, it can be observed that there is a direct relationship between Pb^{2+} concentration and TAA concentration because the more homogenous composites with the smallest particles were obtained in the lowest Pb^{2+} condition and the highest TAA concentration condition or in the intermediate Pb^{2+} condition and the lowest TAA concentration condition.

Acknowledgment

V. H. F. thanks the Conselho Nacional de Desenvolvimento Científico e Tecnológico (CNPq, Brazil) for master degree fellowship. T. S. P. C. thanks the Coordenação de Aperfeiçoamento de Pessoal de Nível Superior (CAPES, Brazil) for doctorate fellowship. A. F. R. acknowledges the financial support given by CNPq, CAPES, Instituto de Ciência, Tecnologia e Inovação em Materiais Complexos Funcionais (INOMAT) and Fundação Araucária (Brazil).

References

1. Algar, W. R.; Tavares, A. J.; Krull, U. J.; *Anal. Chim. Acta* **2010**, *673*, 1.
2. Datta, N. K.; Ghosh, M.; *Mater. Chem. Phys.* **2011**, *126*, 693.
3. Mntungwa, N.; Rajasekhar, P. V. S. R.; Revaprasadu, N.; *Mater. Chem. Phys.* **2011**, *126*, 500.
4. Lou, S.; Zhou, C.; Wang, H.; Shen, H.; Cheng, G.; Du, Z.; Zhou, S.; Li, L. S.; *Mater. Chem. Phys.* **2011**, *128*, 483.
5. Alivisatos, A. P.; *Science, New Series* **1996**, *271*, 933.

6. Lin, W.; Fritz, K.; Guerin, G.; Bardajee, G. R.; Hinds, S.; Sukhovatkin, V.; Sargent, E. H.; Scholes, G. D.; Winnik, M. A.; *Langmuir* **2008**, *24*, 8215.
7. Ferrer, J. C.; Salinas-Castillo, A.; Alonso, J. L.; Ávila, S. F.; Mallavia, R.; *Mater. Chem. Phys.* **2010**, *122*, 459.
8. Blanco-Canosa, J. B.; Medintz, I. L.; Farrell, D.; Mattoussi, H.; Dawson, P. E.; *J. Am. Chem. Soc.* **2010**, *132*, 10027.
9. Mansur, H. S.; Mansur, A. A. P.; *Mater. Chem. Phys.* **2011**, *125*, 709.
10. Kunita, M. H.; Girotto, E. M.; Radovanovic, E.; Gonçalves, M. C.; Ferreira, O. P.; Muniz, E. C.; Rubira, A. F.; *Appl. Surf. Sci.* **2002**, *202*, 223.
11. Goncalves, R. H.; Schreiner, W. H.; Leite, E. R.; *Langmuir* **2010**, *26*, 11657.
12. Cao, J.; Zhu, H.; Deng, D.; Xue, B.; Tang, L.; Mahounga, D.; Qian, Z.; Gu, Y.; *J. Biomed. Mater. Res. Part A* **2012**, *100*, 958.
13. Strasfeld, D. B.; Dorn, A.; Wanger, D. D.; Bawendi, M. G.; *Nano Lett.* **2012**, *12*, 569.
14. Kunita, M. H.; Girotto, E. M.; Radovanovic, E.; Gonçalves, M. C.; Ferreira, O. P.; Muniz, E. C.; Rubira, A. F.; *Appl. Surf. Sci.* **2002**, *202*, 223.
15. Kunita, M. H.; Rinaldi, A. W.; Girotto, E. M.; Radovanovic, E.; Muniz, E. C.; Rubira, A. F.; *Appl. Surf. Sci.* **2006**, *252*, 3707.
16. Silva, R.; Kunita, M. H.; Girotto, E. M.; Radovanovic, E.; Muniz, E. C.; Carvalho, G. M.; Rubira, A. F.; *J. Braz. Chem. Soc.* **2008**, *19*, 1224.
17. Bergbreiter, D. E.; Boren, D.; Kippenberger, A. M.; *Macromolecules* **2004**, *37*, 8686.
18. Silva, R.; Muniz, E. C.; Rubira, A. F.; *Polymer* **2008**, *49*, 4066.
19. Silva, R.; Muniz, E. C.; Rubira, A. F.; *Appl. Surf. Sci.* **2009**, *255*, 6345.
20. Silva, R.; Muniz, E. C.; Rubira, A. F.; *Langmuir* **2009**, *25*, 873.
21. Silva, R.; Pereira, G. M.; Muniz, E. C.; Rubira, A. F.; *Cryst. Growth Des.* **2009**, *9*, 3307.
22. Zhao, N.; Qi, L.; *Adv. Mater.* **2006**, *18*, 359.
23. Yong, K.; Sahoo, Y.; Choudhury, K. R.; Swihart, M. T.; Minter, J. R.; Prasad, P. N.; *Chem. Mater.* **2006**, *18*, 5965.
24. Patel, J. D.; Chaudhur, T. K.; *Mater. Res. Bull.* **2009**, *44*, 1647.
25. Turyanska, L.; Patane, A.; Henini, M.; Hennequin, B.; Thomas, N. R.; *Appl. Phys. Lett.* **2007**, *90*, 101913.
26. Lyakhovetsky, V. R.; Volkov, V. I.; Borshch, A. A.; Brodyn, M. S.; Strashnikova, M. I.; Reznichenko, V. Y.; Kutsenko, A. S.; Maloletov, S. M.; Kuchmy, S. Y.; Kajzar, F.; *Mol. Cryst. Liq. Cryst.* **2005**, *426*, 205.
27. Asunskis, D. J.; Bolotin, I. L.; Hanley, L. J.; *Phys. Chem. Lett.* **2008**, *112*, 9555.
28. Remadevi, T. L.; Preetha, K. C.; *J. Mater. Sci.: Mater. Electron.* **2012**, *23*, 2017.
29. Obaid, A. S.; Mahdi, M. A.; Hassan, Z.; Bououdina, M.; *Mater. Sci. Semicond. Process.* **2012**, *15*, 564.
30. Kotadiya, N. B.; Kothari, A. J.; Tiwari, D.; Chaudhuri, T. K.; *Appl. Phys. A: Mater. Sci. Process.* **2012**, *108*, 819.

Submitted: October 17, 2012
Published online: February 27, 2013